SMGroup

SM Journal of Biomedical Engineering

Research Article

Experimental Test of Olfactory Deposition of Charged Particles under Electric Field Guidance and Bi-directional Breathing Conditions

Jinxiang Xi[1]*, Tyler Demski[1], Yousef Fallatah[1] and Kyle McDonnell[1]

[1]*School of Engineering and Technology, Central Michigan University, USA*

Article Information

Received date: Mar 16, 2016
Accepted date: May 27, 2016
Published date: May 30, 2016

***Corresponding author**

Jinxiang Xi, School of Engineering and Technology, Central Michigan University, USA, Email: xi1j@cmich.edu

Keywords Olfactory Mucosa; Charged Particles; Electric Field Guidance; Point-Release; Nose-to-Brain Delivery

Abstract

Background: The complex structure of the nasal cavity filters most of the nasally administered aerosols and prevents effective drug delivery to the olfactory region. Due to low medication bioavailability in this region, treatment of brain tumors with direct nose-to-brain drug delivery is still not feasible.

Objectives: The objective of this study is to experimentally evaluate the performance of a hybrid delivery method in an image-based nasal model by leveraging the advantages of both the bi-directional delivery strategy and the electric field guidance of charged particles.

Methods: A sectional hollow nasal cast model was developed from an anatomically accurate nasal airway model that allowed direct quantification of olfactory deposition and visualization of regional deposition distributions. Influences of different electric field strengths and two delivery strategies (normal and bi-directional) on the olfactory delivery were tested.

Results: Results show that olfactory deposition is very sensitive to the voltage of the electrode close to the olfactory region. For both the normal and bi-directional deliveries, electric field guidance resulted in a significant increase (3–5 times) in deposition in the olfactory region. The olfactory deposition with electric guidance was 1.6 times higher when using the bidirectional method than under normal breathing conditions.

Conclusions: Results of this study indicate that the combination of electric field guidance of charged particles and the bi-directional delivery strategy is promising to deliver significantly improved medications to the olfactory region.

Introduction

Intranasal olfactory drug delivery provides a noninvasive practical method of bypassing the blood-brain-barrier and represents a desirable alternative to deliver medications to the brain [1-3]. However, many challenges exist that prevent effective drug delivery to the olfactory region. The complex structure of the nasal cavity filters most of the nasally administered aerosols [4]. Furthermore, medications need to penetrate high and deep enough to reach the olfactory region due to its uppermost location in the nasal cavity [5,6]. The lack of control over the particle trajectory after release is another reason for low olfactory doses. After a particle is released, its path is completely dictated by the intranasal airflow field through a concurrent mechanism of particle inertia, drag, weight, and Brownian force if particle size is submicrometer. The majority of particles will be lost in the nasal valve or turbinate before making their way to the olfactory region. Due to the low bioavailability of administered medications, direct nose-to-brain drug delivery is still not clinically feasible [6,7].

Many studies have explored new strategies to enhance drug delivery to the olfactory region. These efforts can be classified into three categories: to increase upper posterior deposition of nasal sprays by minimizing nasal valve filtration [8-11], to disperse nebulized aerosols across the nose using pulsating flows [12-15], and to actively control particle trajectories with electromagnetic forces [16-19]. Studies in the first category with nasal spray pumps were generally the earliest experiments conducted. Wang, et al. [20] inserted a nasal spray catheter into the nasal cavity and administered drugs below the olfactory epithelium. This method has not found broad applications due to potential bruising to the wall tissues when inserting the catheter. A less invasive approach was attempted by using narrow plume sprays to overcome the nasal resistance and transport drugs to the upper nose and olfactory region [21]. However, drug losses to the nasal valve were large and enhancements of the olfactory delivery were limited. To enhance the olfactory ventilation, Hoekman and Ho [22] applied a vortex flow to the narrow spray plume and demonstrated improved olfactory dosages in rats than using the nasal drop. However, trials in human subjects or *in vitro* casts have not been reported. The second category involved imposing a pulsating flow

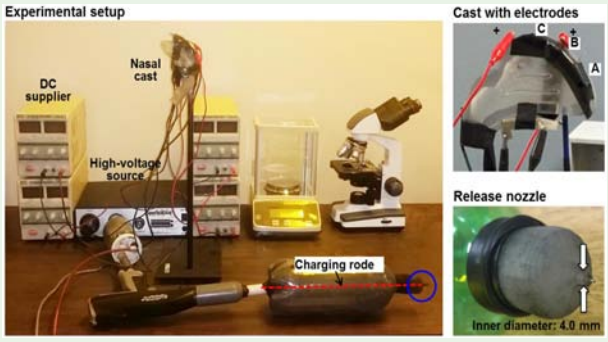

Figure 1: Experimental setup of electric-guided olfactory drug delivery.

onto nebulized aerosols and has been demonstrated to deliver more aerosols to the sinus and possibly to the olfactory region [12,23,24]. However, pulsating flows are prone to more evenly coating the nose surface and may not be suitable for targeted drug deliveries of neurological pharmaceuticals [25]. Moreover, the delivery efficiency to the olfactory region with pulsating flows may not be high enough to be considered clinically significant [26,27]. Charged particles have been suggested for targeted delivery to the human nose and lungs [28-30]. Enhanced deposition due to particle electrostatic charges has been demonstrated in human subjects, *in vitro* airway replicas, and numerical modeling [31-37]. Realizing that the low olfactory doses are primarily due to the lack of control over particle motions after their release, Xi, et al. [38] evaluated the feasibility of using external electric field to control the motion of charged particles in the nose. Results from numerical studies have shown significant enhancements of drug delivery to the olfactory region with an appropriate electric field [38]. Complementary *in vitro* tests also qualitatively demonstrated higher deposition in the olfactory region [39]. However, no quantitative results of the olfactory doses were obtained in the above study.

One issue of intranasal drug delivery of nebulized droplets or small particles is the unwanted dosages to the lungs. One strategy to address this issue is the bi-directional delivery method, which administers medications into one nostril when the patient blows into the apparatus [40]. This method takes advantage of the oropharynx closing due to uplifting the soft palate during exhalation through the mouth. As a result, particle penetration into the lungs can be avoided. Moreover, the particles enter one nostril and exit from the other, which allows an increased period of time for drug deposition. This method did show an increase in medications depositing in the nasal cavity, but failed to provide a practical way of dispensing an appreciable amount of medications to the olfactory region [41,42]. It is hypothesized that by combining the particle electric guidance with the bi-directional strategy, the olfactory dosage can be further enhanced.

The objective of this study is to experimentally assess the performance of a hybrid delivery protocol that leverages the advantages of both electric field guidance and bi-directional delivery strategy in an image-based nasal model. There are three specific aims: (1) to characterize the variation of the olfactory dosage with the electric field strength, (2) to quantify the increase in the olfactory dosage of the proposed method than the control case (without electric guidance),and (3) to quantify the difference of electric-guided olfactory dosages between normal and bi-directional delivery methods.

Methods and Materials

In vitro test platform

The test platform for the electric-guided intranasal delivery has four components: a particle charging apparatus, a three-dimensional replica of an average human nasal cavity, an external electric field generator, and measurement instruments (Figure 1). A Spectracoat™ ES02-WC powder coating system (Powder System Solutions, Nolensville, TN) was reverse-engineered to charge dry powders. Copper plates connected to a Direct Current (DC) power supply (MPJA, Lake Park, FL) were used to generate the required electric field. An electron scale was used to measure particle weights and a multimeter was used to measure electric properties. A microscope (AmScope B120C-E1) was used to estimate the diameter of the charged particles. Details of the sectional nasal cast preparation and experimental procedures are described below.

Sectional nasal cast

A sectional nasal cast was developed that allows quantitative measurement of regional deposition as well as direct visualization of deposition distributions. The nasal airway geometry that had been reconstructed from head MRI scans of a 53-year-old male [43,44] was used to prepare the *in vitro* nasal cast replicas (Figure 2a). Magics (Materialise, Ann Arbor, MI) was used to generate the nasal wall with a finite thickness of 4 mm. The nasal cast was divided into several parts, such as the nasal vestibule and valve, turbinate, and nasopharynx (Figure 2b). A step-shaped groove was designed at each end of the cast parts for easy assembly and proper sealing (Figure 2b). To visualize deposition patterns inside the nose, the vestibule-turbinate was further divided into two parts along the top ridge of the right nasal septum to show the internal structures of the right side of the nasal passage. To quantitatively measure drug dosages in the olfactory region, an area that represents the olfactory mucosa was cut out from the upper turbinate, as shown in Figure 2b. An in-house 3-D printer with are solution of 16 μm (0.0006 in) (Stratasys Objet30 Pro, Northville, MI) was used to build the nose replicas using polypropylene (Veroclear, Northville, MI), which is transparent and allows for a smooth surface.

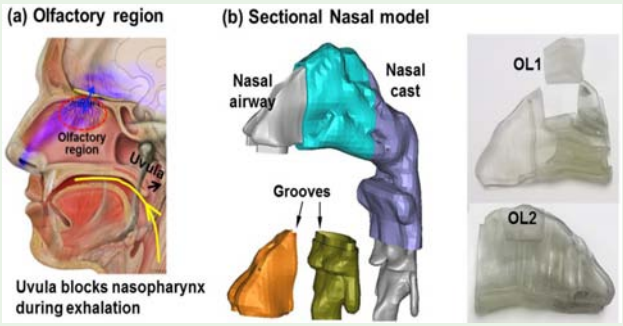

Figure 2: Olfactory region and sectional nasal model. **(a)** The olfactory mucosa is located at the upper nasal cavity and is connected with the brain. **(b)** A nose cast with a constant shell thickness was developed from an MRI-based nasal airway model. The cast was divided into different sections to measure the regional deposition and was cut open to visualize the deposition distributions inside the nose. The olfactory region was also separated to measure the olfactory dosage. Grooves were designed at the connections for easy assembly and good sealing.

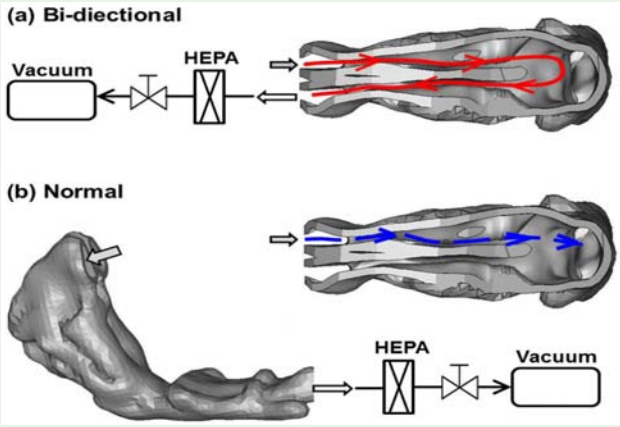

Figure 3: Two delivery strategies: **(a)** bidirectional, and **(b)** normal. In both cases, particles are administered into the right-side nostril.

Experimental procedures

The apparatus used to charge and distribute solid particles was a modified Spectracoat™ ES02-WCpowder-coating system (Nolensville, TN) (Figure 1). Dry powders (Matte Black Powder Coat Paint) of approximately 30 μm in diameter were used in this study. The modification made to the powder coating system integrated a charging reservoir (i.e., a two-liter bottle) to the nozzle of the charging gun. An additional metal wire was added to extend the charging rod to the reservoir exit, with the wire's length being parallel with the direction of the flow of solid particles. The voltage to the rod was charged with a high negative potential. A high voltage source (Spectracoat coating system) was used which can provide an adjustable 0–100 kV potential output. The solid particles were distributed out of a 4mm diameter nozzle (Figure 1, right lower panel), and subsequently distributed into a multi-sectional nasal cast replica. Different parts of nasal casts were assembled and held together by a strip-caulk (3M, part NO. 05135-68578). Strip-caulk and electrical tape were used to attach the nose replica to a metal stand. Similarly, three copper-plated electrodes (A, B, C) were attached to the bridge of the nose replica (Figure 1, upper right panel) and one copper plated electrode was attached to the bottom of the replica. The bottom electrode will act as the ground electrode. In clinical applications, this ground electrode will be positioned in the patient's mouth. Because the electrodes are all enclosed by insulations, there is no direct contact between the electrodes and skin. Therefore, it is safe to the patient even though 70 V or higher voltages are used. The solid particles were distributed from the powder coat gun for 20 seconds per trial. For bi-directional deliveries, the bottom of the pharynx was blocked to simulate the uplifted soft palate, while particles were administered into one nostril and exited through the other (Figure 3a). In contrast, for normal deliveries, particles were administered into one nostril and exited through the nasopharynx (Figure 3b). A vacuum (Robinair 3 CFM, Warren, MI) was connected to the exit in each case to simulate the inhalation. The volumetric flow rate was monitored by an in-line flow meter (Omega, FL-510, Stamford, CT).

Table 1: Sensitivity analysis of electrode voltage magnitudes.

Electrode	E1	E2	E3	E4	E5
A (V)	15	15	15	20	20
B (V)	25	25	30	30	30
C (V)	50	60	60	60	70
Nasal dosage (g)	0.019	0.031	0.032	0.040	0.053

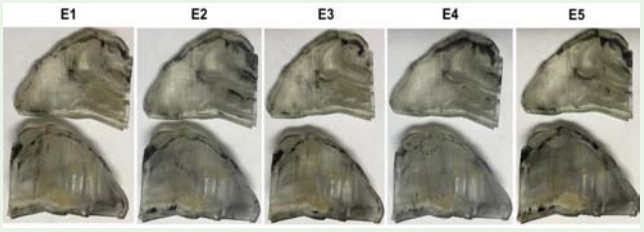

Figure 4: Visualization of deposition patterns of the five electrode combinations.

Statistical analysis

The variable of interest in this study was the ratio of the olfactory dosage to the vestibule-turbinate dosage (i.e., olfactory-nasal dosage ratio). Results were represented as the main ± Standard Deviation (SD), with SD being calculated from five trials for each scenario. Minitab 17 analysis software (State College, PA) was used to analyze deposition results to determine the importance of different factors. One-Way Analysis of Variance (ANOVA) and Tukey's method with stacked data were used to evaluate the sample variability. The difference was considered statistically significant if the *p-value* was < 0.05.

Results

Sensitivity analysis of electrode voltages

Multiple trials were conducted to find a practical combination of electrode voltages that are capable of guiding particles to the olfactory region. Deposition distributions in the nasal cavity with 20 seconds particle release are displayed in Figure 4 for five electrode combinations (E1–E5), as listed in Table 1. Comparison of the nasal (vestibule-turbinate) dosages among the five electrode combinations is shown in Figure 5. The voltage combination in the first trial (E1) was 15V, 25V, and 50V at nodes A, B, and C respectively. From Figure 4, there was some build-up of particles near the olfactory region. The deposited dosage in the vestibule-turbinate region was measured as 0.019g (Figure 5a). Furthermore, there was an appreciable amount of particles deposited in the rear airway passages (nasopharynx) (Figure 5b).

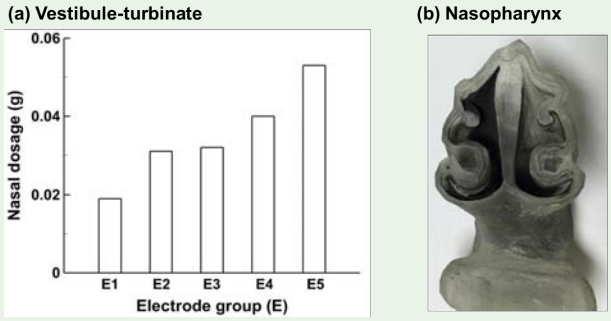

Figure 5: Nasal deposition: **(a)** nasal (vestibule-turbinate) dosages for the five electrode combinations (E1–E5), **(b)** deposition in the nasopharynx.

Figure 6: Deposition pattern in the right nasal passage and nasopharynx under bi-directional breathing conditions.

In the second trial (E2), the voltage at node C was increased from 50V to 60Vwhile keeping the same voltages at nodes A and B, in hope that it would increase particle build-up in the olfactory region and decrease the particle deposition in the rear air passageway. As expected, there was an increased build-up of particles in the olfactory region (Figure 4). Particle deposition in the rear air passage way also decreased. The deposited dosage in the vestibule-turbinate region was measured as 0.031g (Figure 5a).

In the third trial (E3), increasing the voltage at node B from 25Vto 30V and keeping the same voltages at nodes A and C did not have a strong effect on the particle deposition, which slightly increased to 0.032g. The deposition patterns also appeared similar between E2 and E3.

In the fourth trial (E4), the voltage at node A was increased from 15V to 20V and those at nodes B and C were kept at the same voltages. This electrode voltage combination yielded an improved particle deposition of 0.040g in comparison to 0.032g in E3 (Figure 5a). The increased voltage at node A helped minimizes particle deposition in the rear air passageway, hence leading to increased vestibule-turbinate dosage. Particle deposition in the olfactory region also showed improvement (Figure 4, E4). The underlying mechanism was hypothesized to be the decreased particle losses in the nasal valve region, where node A was located.

Finally in the fifth trial (E5), increasing the voltage at node C from 60V to 70V and keeping nodes A and B with the same voltages of 20V and 30V respectively resulted in a higher particle deposition of 0.053g (Figure 5a). The large increase in the olfactory dosage suggested a high sensitivity of the olfactory dosage to the magnitude of node C, which is near the olfactory region. Therefore, the electrode combination in E5 was used in the following tests for both bi-directional and normal deliveries.

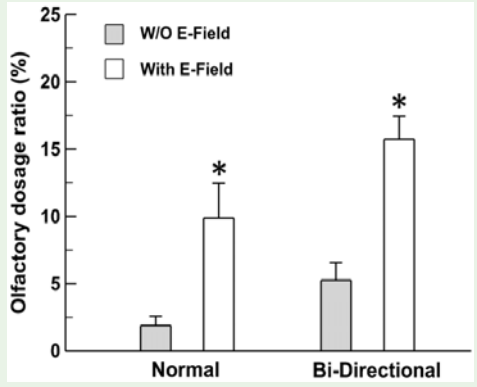

Figure 7: Comparison of the olfactory-to-nasal dosage ratio with and without electric field guidance for the normal and bi-directional delivery strategies.*p-*value*< 0.05.

Bi-directional delivery *vs.* normal delivery

To quantify the effects of the electric field guidance on the olfactory drug delivery, a four-piece nasal cast was implemented, with two small pieces representing the olfactory region, and the other two large pieces representing the nose (vestibule-turbinate region). In each test, masses of the two pieces of the olfactory region and the two larger pieces of the nose were measured separately before and after the test. By doing so, the deposition rate in the olfactory region (i.e., the ratio of the olfactory dosage over the nasal dosage) was calculated.

The distribution of particle deposition using the bi-directional method is shown in Figure 6. Particles accumulated in high concentrations in the upper nose of the right nasal passage, indicating effective electric field guidance of charged particles to the olfactory region. It was also noted that particle deposition in the two passages were apparently different (right panel, Figure 6). In the right passage, particle deposition was more uniformly distributed and a large portion of particles were pulled towards the electrodes, primarily electrode C. By contrast, the majority of particles in the left passage deposited in the inferior nose while much fewer particles reached the upper nose, presumably due to the gravitational effect.

Figure 7 shows the comparison of the olfactory-to-nasal dosage ratio between the cases with and without the electric field guidance. The particle releasing time is 20 seconds and the results are presented as the mean ± SD from five trials. Significantly improved depositions were obtained with the electric field guidance for both normal and bi-directional delivery strategies. There was an increase in olfactory deposition in the normal delivery by a factor of 5 and in the bi-directional delivery by a factor of 3.

The effects of delivery strategy were examined by comparing the olfactory delivery enhancements between the normal and bi-directional strategies. In the absence of an electric field, the bi-directional method resulted in an increase in the olfactory delivery by a factor of 2.8 compared to the normal breathing condition. However, with the electric field guidance the olfactory enhancement due to the bi-directional method was only 1.6 times greater than that of the normal breathing condition.

Discussion and Summary

In this study, a range of 0-70V was used in designing the electrode layout. As observed in the first experiment, olfactory deposition was most sensitive to the electric potential at node C because of its proximity to the olfactory region. It is expected that an increase in node C potential will further enhance the deposition to the olfactory region. However, the benefits from an increased voltage at node C decrease as its voltage becomes larger. Considering that node C can only be positioned anterior to the olfactory region due to the limitations of human head anatomy, too large of a voltage at node C will attract particles to the nasal surface ahead of the olfactory mucosa, decreasing the dosages that can reach the olfactory region. In this *in vitro* experimental study, only a limited number of node voltages were tested. Numerical modeling and optimization were

more appropriate to identify the optimal voltages at each node. Nonetheless, the measurements in this study exhibited significantly enhanced olfactory deposition with applied electric field guidance and demonstrated the potential of electric field guidance to improve olfactory drug deliveries.

Different delivery strategies respond differently to the electric field guidance. The olfactory dosage with the bi-directional method was higher than that of the normal method, but was lower than twice of the dosage of the normal method. In the bi-directional method, a particle traveled through both nasal passages in series and doubled its course when compared to the normal delivery method. However, due to the large particle size (~30μm) considered in this study, only a small fraction of the particles that had escaped filtration of the first nasal passage could change direction sharply enough to enter the second nasal passage. Therefore, more particles are expected to deposit in the first passage than in the second passage when using the bi-directional technique. The higher flow resistance in the first passage and possibly the expansion of the nasal cavity due to the high resistance may also contribute to higher deposition fractions in the first passage. However, further studies are needed to validate this theory.

For both the normal and bi-directional deliveries, electric field guidance of charged particles yielded significantly higher olfactory depositions than delivery methods without electric field guidance. In contrast, deposition enhancements were relatively limited in our previous attempts to improve olfactory dosages by optimizing the airflow and particle release [45]. Such attempts tried to find the particles that are more likely to make their way to the target and use them as the initial condition, anticipating that particles can find their way back to the target when released from the nostril. However, no active control can be exerted on the particle once it is released into the nasal cavity. Instead, aerodynamic drag and gravity are the two major forces that dictate the course of the particle. As a result, only limited enhancement to olfactory dosage has been obtained so far [45]. Such examples include adaptation of existent nebulizers or nasal sprays. Xi, et al. [46] experimentally evaluated the effects of the release area and release position of particles and found limited deposition increase in the olfactory region. In addition, nasal sprays were found to lose substantial fractions of administered particles in the anterior nose and may not be suitable for precise targeted drug delivery. By contrast, the electric guidance technique exerts an extra field force (electric force) on the charged particles. In principle, it is possible to actively control the particle trajectory through electric field guidance so that it can avoid the nasal walls, navigate an obstacle or corner, and change the direction to enter an otherwise poorly ventilated space. In doing so, an accurate knowledge of the intended path of a particle is required beforehand. This requirement, however, is not unlikely considering the advances in medical imaging techniques. With MRI or CR scans of a patient, it is now a routine procedure to reconstruct the 3D nasal airway geometry and find the optimal drug path leading to optimal olfactory dosages, as demonstrated in this and other studies [38].

In this study, the olfactory deposition was represented as the ratio of the olfactory dosage to the vestibule-turbinate dosage to facilitate comparisons among different tests. Deposition in the nasopharynx was not considered due to the materials and instruments used in this study. Connection between the nasal cast and vacuum was secured by strip-caulk (3M, 05135068578), which cannot be completely removed after testing and therefore, cannot accurately measure the weight difference before and after the test. Nonetheless, the ratio of the olfactory dosage to the vestibule-turbinate dosage gives a reasonable indication for drug delivery efficiency to the olfactory region.

One unexpected observation in this study was that there was greater particle build-up throughout the nasal cavity when the nose cast had a wet surface (i.e., had not dried in the oven). This observation may be attributed to either the modification of particle charges by the relative humidity [47,48] or the hygroscopic growth of the particles [49-51]. To minimize the complications from the environmental humidity and surface wetness, two procedures were carried out. First, after each test the nasal cast was cleaned with a power washer, pre-dried with compressed air, and then dried in an oven of 125 $^{\circ}$F for 30 minutes to remove moisture inside the cast. Second, the cast was left in the air for additional 30 minutes to let the cast become fully equilibrated with the environment. It is also reminded that *in vivo* nose surfaces are wet, with a relative humidity of approximately 99.5%. Even though the above two procedures did not mimic the *in vivo* condition, they ensured that all tests were conducted with comparable cast surface conditions. Further tests with simulated *in vivo* surface conditions are needed.

The nasal casts in this study were prepared using polypropylene, which has a lower relative permittivity (i.e., 2.2-2.36) from that of the nasal bones (i.e., 6.47) [39]. The electric field and resultant delivery doses are expected to differ between *in vitro* and *in vivo* tests. In light of the higher relative permittivity of nasal cartilages than the plastic, lower olfactory doses at are expected in clinical applications. Likewise, to achieve similar doses in clinical application, higher electrode voltages or higher particle charges are needed.

Other limitations in this study include the usage of steady flows, rigid nose cast, nose replicas based on one subject, and large particle size. Influences from tidal breathing [52] and compliant walls [53] may alter particle motions regional dosage. The nose replicas were developed from one subject and did not account for discrepancies due to age, gender, race, weight, or height. Dry powders of 30 μm were tested in this study, which are much larger than typical intranasal pharmaceuticals (2–5 μm) and are expected to be less responsive to electric field guidance. Further studies with particles of smaller sizes are warranted.

In summary, deposition of charged particles under the influence of an external electric field was measured in both the nose and the olfactory region. Different electric field strengths and delivery strategies were tested. Specific findings are:

1. Among the three electrodes (A, B and C) considered, olfactory deposition showed the highest sensitivity to node C, which is closest to the olfactory region, followed by node A (above the nasal valve), and node B (the middle electrode).

2. For both the normal and bi-directional deliveries, electric field guidance resulted insignificantly higher deposition in the olfactory region. There was a 5.2 fold increase for the normal delivery strategy and a 3.0 fold increase for the bi-directional strategy.

3. Particle deposition enhancement in the olfactory region was higher when using the bi-directional method than that when using the normal breathing method. The electric guided olfactory deposition efficiency under bi-directional breathing was1.6 times that under normal breathing conditions.

Acknowledgement

This study was funded by Central Michigan University Innovative Research Grant P421071 and Early Career Award P622911.

References

1. Pardeshi CV, Belgamwar VS. Direct nose to brain drug delivery via integrated nerve pathways bypassing the blood-brain barrier: an excellent platform for brain targeting. Expert Opin Drug Deliv. 2013; 10: 957-972.
2. Mistry A, Stolnik S, Illum L. Nanoparticles for direct nose-to-brain delivery of drugs. Int J Pharm. 2009; 379: 146-157.
3. Illum L. Is nose-to-brain transport of drugs in man a reality? J Pharm Pharmacol. 2004; 56: 3-17.
4. Xi J, Longest PW. Numerical predictions of submicrometer aerosol deposition in the nasal cavity using a novel drift flux approach. Int J Heat Mass Tran. 2008; 51: 5562-5577.
5. Misra A, Kher G. Drug delivery systems from nose to brain. Curr Pharm Biotechnol. 2012; 13: 2355-2379.
6. Mittal D, Ali A, Md S, Baboota S, Sahni JK, Ali J. Insights into direct nose to brain delivery: current status and future perspective. Drug Delivery. 2014; 21: 75-86.
7. Ong W-Y, Shalini S-M, Costantino L. Nose-to-Brain Drug Delivery by Nanoparticles in the Treatment of Neurological Disorders. Curr Med Chem. 2014; 21: 4247-4256.
8. Lam K, Tan BK, Lavin JM, Meen E, Conley DB. Comparison of Nasal Sprays and Irrigations in the Delivery of Topical Agents to the Olfactory Mucosa. Laryngoscope. 2013; 123: 2950-2957.
9. Vasa DM, O'Donnell LA, Wildfong PLD. Influence of Dosage Form, Formulation, and Delivery Device on Olfactory Deposition and Clearance: Enhancement of Nose-to-CNS Uptake. J Pharm Innov. 2015; 10: 200-210.
10. Hummel T, Rothbauer C, Pauli E, Kobal G. Effects of the nasal decongestant oxymetazoline on human olfactory and intranasal trigeminal function in acute rhinitis. Eur J Clin Pharmacol. 1998; 54: 521-528.
11. El Taoum KK, Xi J, Kim JW, Berlinski A. In Vitro Evaluation of Aerosols Delivered via the Nasal Route. Respir Care. 2015; 60: 1015-1025.
12. Moeller W, Schuschnig U, Celik G, Muenzing W, Bartenstein P, Haeussinger K, et al. Topical drug delivery in chronic rhinosinusitis patients before and after sinus surgery using pulsating aerosols. PLoS ONE. 2013; 8: e74991.
13. Moeller W, Saba GK, Haeussinger K, Becker S, Keller M, Schuschnig U. Nasally inhaled pulsating aerosols: lung, sinus and nose deposition. Rhinology. 2011; 49: 286-291.
14. Granqvist S, Sundberg J, Lundberg JO, Weitzberg E. Paranasal sinus ventilation by humming. J Acoust Soc Am. 2006; 119: 2611-2617.
15. Durand M, Le Guellec S, Pourchez J, Dubois F, Aubert G, Chantrel G, et al. Sonic aerosol therapy to target maxillary sinuses. Eur Ann Otorhinolaryngol Head Neck Dis. 2012; 129: 244-250.
16. Xi J, Zhang Z, Si X. Improving intranasal delivery of neurological nanomedicine to the olfactory region using magnetophoretic guidance of microsphere carriers. Int J Nanomedicine. 2015; 10: 1211-1222.
17. Xi J, Yuan JE, Si XA. Simulation study of electric-guided delivery of 0.4 μm monodisperse and polydisperse aerosols to the ostiomeatal complex. Comput Biol Med. 2016. 72: 1-12.
18. Xi J, Zhang Z, Si XA, Yang J, Deng W. Optimization of magnetophoretic-guided drug delivery to the olfactory region in a human nose model. Biomech Model Mechanobiol. 2015 (In press).
19. Xi J, Yuan JE, Si XA, Hasbany J. Numerical optimization of targeted delivery of charged nanoparticles to the ostiomeatal complex for treatment of rhinosinusitis. Int J Nanomedicine. 2015; 10: 4847-4861.
20. Wang J, Bentz J, Anderson R. Nasal device for delivery to the olfactory region. US 20070119451 A1. 2007.
21. Gizurarson S. A Method for administration of active substances to the olfactory region. CA 2298596 A1. 2003.
22. Hoekman JD, Ho RJY. Enhanced analgesic responses after preferential delivery of morphine and fentanyl to the olfactory epithelium in rats. Anesth Analg. 2011; 113: 641-651.
23. Leclerc L, Pourchez J, Aubert G, Leguellec S, Vecellio L, Cottier M, et al. Impact of airborne particle size, acoustic airflow and breathing pattern on delivery of nebulized antibiotic into the maxillary sinuses using a realistic human nasal replica. Pharm Res. 2014; 31: 2335-2343.
24. Maniscalco M, Sofia M, Weitzberg E, Lundberg JO. Sounding airflow enhances aerosol delivery into the paranasal sinuses. Eur J Clin Invest. 2006; 36: 509-513.
25. Sato Y, Hyo N, Sato M, Takano H, Okuda S. Intranasal distribution of aerosols with or without vibration. Zeitschrift fuer Erkrankungen der Atmungsorgane. 1981; 157: 276-280.
26. Laube BL. Devices for aerosol delivery to treat sinusitis. J Aerosol Med. 2007; 20: 5-18.
27. Albu S. Novel drug-delivery systems for patients with chronic rhinosinusitis. Drug Des Dev Ther. 2012; 6: 125-132.
28. Wilson IB. The deposition of charged particles in tubes, with reference to the retention of therapeutic aerosols in the human lung. J Colloid Sci. 1947; 2: 271-276.
29. Bailey AG, Hashish AH, Williams TJ. Drug delivery by inhalation of charged particles. J Electrostat. 1998; 44: 3-10.
30. Wong J, Chan H-K, Kwok PCL. Electrostatics in pharmaceutical aerosols for inhalation. Ther Deliv. 2013; 4: 981-1002.
31. Yu CP. Theories of electrostatic lung deposition of inhaled aerosols. Ann Occup Hyg. 1985; 29: 219-227.
32. Ali M, Reddy RN, Mazumder MK. Electrostatic charge effect on respirable aerosol particle deposition in a cadaver based throat cast replica. J Electrostat. 2008; 66: 401-406.
33. Scheuch G, Gebhart J, Roth C. Uptake of electrical charges in the human respiratory tract during exposure to air loaded with negative ions. J Aerosol Sci. 1990; 21: 439-442.
34. Azhdarzadeh M, Olfert JS, Vehring R, Finlay WH. Effect of electrostatic charge on oral-extrathoracic deposition for uniformly charged monodisperse aerosols. J Aerosol Sci. 2014; 68: 38-45.
35. Melandri C, Tarroni G, Prodi V, De Zaiacomo T, Formignani M, Lombardi CC. Deposition of charged particles in the human airways. J Aerosol Sci. 1983; 14: 657-669.
36. Hashish AH, Bailey AG, Williams TJ. Selective deposition of pulsed charged aerosols in the human lung. J Aerosol Med. 1994; 7: 167-171.
37. Ali M. Engineered Aerosol Medicine and Drug Delivery Methods for Optimal Respiratory Therapy. Respir Care. 2014; 59: 1608-1610.
38. Xi J, Si X, Gaide R. Electrophoretic particle guidance significantly enhances olfactory drug delivery: a feasibility study. PLoS ONE. 2014; 9: e86593.
39. Xi J, Yuan J, Alshaiba M, Cheng D, Firlit Z, Johnson A, et al. Design and testing of electric-guided delivery of charged particles to the olfactory region: experimental and numerical studies. Curr Drug Deliv. 2016; 13: 265-274.
40. Djupesland PG, Skretting A, Winderen M, Holand T. Bi-directional nasal delivery of aerosols can prevent lung deposition. J Aerosol Med Pulm Drug Deliv. 2004; 17: 249-259.
41. Luthringer R, Djupesland PG, Sheldrake CD, Flint A, Boeijinga P, Danjou P, et al. Rapid absorption of sumatriptan powder and effects on glyceryl trinitrate model of headache following intranasal delivery using a novel bi-directional device. J Pharm Pharmacol. 2009; 61: 1219-1228.

42. Djupesland PG, Docekal P, Czech Migraine Investigators G. Intranasal sumatriptan powder delivered by a novel breath-actuated bi-directional device for the acute treatment of migraine: A randomised, placebo-controlled study. Cephalalgia. 2010; 30: 933-942.

43. Xi J, Longest PW. Characterization of submicrometer aerosol deposition in extrathoracic airways during nasal exhalation. Aerosol Sci Technol. 2009; 43: 808-827.

44. Zhou Y, Guo M, Xi J, Irshad H, Cheng Y-S. Nasal deposition in infants and children. J Aerosol Med Pulm Drug Deliv. 2014; 27: 110-116.

45. Si X, Xi J, Kim J, Zhou Y, Zhong H. Modeling of release position and ventilation effects on olfactory aerosol drug delivery. Respir Physiol Neurobiol. 2013; 186: 22-32.

46. Xi J, Yuan J, Zhang Y, Nevorski D, Wang Z, Zhou Y. Visualization and quantification of nasal and olfactory deposition in a sectional adult nasal airway cast. Pharm Res. 2016; 33: 1527-1541.

47. Kwok PCL, Chan H-K. Effect of relative humidity on the electrostatic charge properties of dry powder inhaler aerosols. Pharmaceutical Research. 2008; 25: 277-288.

48. Young PM, Sung A, Traini D, Kwok P, Chiou H, Chan H-K. Influence of humidity on the electrostatic charge and aerosol performance of dry powder inhaler carrier based systems. Pharm Res. 2007; 24: 963-970.

49. Longest PW, Xi JX. Condensational growth may contribute to the enhanced deposition of cigarette smoke particles in the upper respiratory tract. Aerosol Sci Technol. 2008; 42: 579-602.

50. Kim JW, Xi J, Si XA. Dynamic growth and deposition of hygroscopic aerosols in the nasal airway of a 5-year-old child. Int J Numer Method Biomed Eng. 2013; 29: 17-39.

51. Xi J, Kim J, Si XA, Zhou Y. Hygroscopic aerosol deposition in the human upper respiratory tract under various thermo-humidity conditions. J Environ Sci Health A Tox Hazard Subst Environ Eng. 2013; 48: 1790-1805.

52. Xi J, Longest PW, Martonen TB. Effects of the laryngeal jet on nano- and microparticle transport and deposition in an approximate model of the upper tracheobronchial airways. J Appl Physilo. 2008; 104: 1761-1777.

53. Berg EJ, Weisman JL, Oldham MJ, Robinson RJ. Flow field analysis in a compliant acinus replica model using Particle Image Velocimetry (PIV). J Biomech. 2010; 43: 1039-1047.